

# 734. Field-circuit modeling of AMB system for various speeds of the rotor

Jan Zimon<sup>1</sup>, Bronisław Tomczuk<sup>2</sup>, Dawid Wajnert<sup>3</sup>

Opole University of Technology, Department of Industrial Electrical Engineering  
Prószkowska str. 76, 45-758 Opole, Poland

E-mail: <sup>1</sup>j.zimon@po.opole.pl, <sup>2</sup>b.tomczuk@po.opole.pl, <sup>3</sup>dawid.wajnert@op.pl

(Received 11 September 2011; accepted 14 February 2012)

**Abstract.** The non-symmetrical twelve poles active magnetic bearing (AMB12) actuator has been considered. We also included the control system for the computer simulation. We have used the field-circuit method modeling included under various speed of the rotor. The electromechanical equation system has been solved taking into account the integral parameters obtained from Finite Element Method (FEM) analysis of the magnetic field. We verified the calculations by the measurement tests under various values of the rotational speed of the AMB rotor. A good agreement has been achieved.

**Keywords:** field-circuit method, active magnetic bearing, digital control system.

## Introduction

Today, the fast rotating machines need safe and reliable bearing systems. Since last thirty years, the new method of magnetic suspension has been developed in many scientific centers. The magnetic bearing technology application can be used for the strategic drives [1].

In recent years, magnetic levitation and suspension have become a realistic realization in the mechatronic systems. The real-time calculations and peripheral functions can be implemented using the digital control algorithms. The current regulators including power electronic inverters could be better designed as since 30 years ago, also. Nowadays, the latest digital processors and field programmable gate arrays allow for creating the A/D converters and 3-phase PWM systems. Mostly, the magnetic bearings have been modeled as the permanently acting forces. They are defined as the functions of rotor displacement and control currents. Additionally, the transfer function of the AMB system is inherently unstable [1], [6]. Thus, for the designing of the controller, the most important task is minimization the rotor eccentricity.

## Active magnetic bearing description

We considered the non-typical 12 poles actuator, which has been invented (including its control system) in the Department of Industrial Electrical Engineering at Opole University of Technology. We called it AMB12, [8]. The actuator consists of two main parts: stator and rotor. Both parts are made from packages laminated from M50-270 [9] carbon steel sheets. The laminated rotor as well as a solid ring for displacement measurements are placed on the solid iron shaft [4], [7], [8]. The stator of the AMB characterizes by non-symmetrical excitation windings and was developed as a vertical working radial bearing, Fig. 1a. The main suspension force and the gravitation one act along the “y” axis, Fig 1b. In Fig. 1a is shown, the diagram of the electromagnet coil connection into four sections, [2], [7]. Two of them create electromagnets acting in “y” axis and two of them create electromagnets acting along “x” axis. Thus, the force acted on bearing shaft is two times higher in vertical direction, then in the horizontal one. This causes non symmetrical distribution of the bearing stiffness in each points of the rotor close to the bearing air gap. The air gap between stator and rotor is 0.5mm under the central position of the shaft. Including the rotor displacement, the operating air gap is limited to the value of 0.3mm [8].

The shaft position is determined by the simple inductance sensors. The contact-less sensors are screwed in the bearing housing and they are perpendicular to rotational axis of the bearing

rotor. Theirs bandwidth is 200 Hz wide. One can add that the measurement range is equal to (0.5÷3) mm and the position controllers are operated with sampling of 1 kHz. The control tasks have been realized with a 32-bit microcontroller LPC2144, which has been manufactured by NXP company. It contains very efficient ARM7TDMI-S core and 256 kB flash memory. The core includes 10-bit A/D converter with maximum conversion frequency 400 kHz and PWM generator based on the single chip. Digital conversion resolution amounts 2.44 μm/bit. The current converter resolution is 60 mA/bit. The AMB windings are supplied with four modules of the PWM switching amplifiers with power of 700 VA per one channel. Each of them consists of single-phase H-bridge circuit, current sensor and over-current control unit. The power amplifiers are controlled by PWM wave with 25 kHz frequency and variable duty cycle. The current measurement is required for sets up of two PI controllers. The sampling frequency of each controller is 10 kHz.

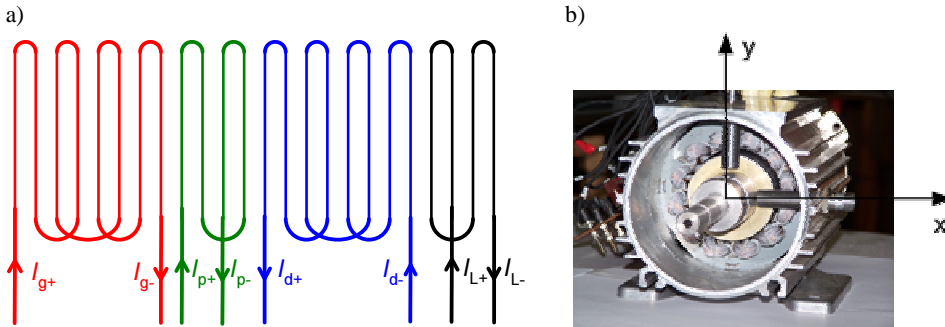


**Fig. 1.** AMB12 winding configuration (a) and opened AMB with displacement sensors (b) view of the AMB12

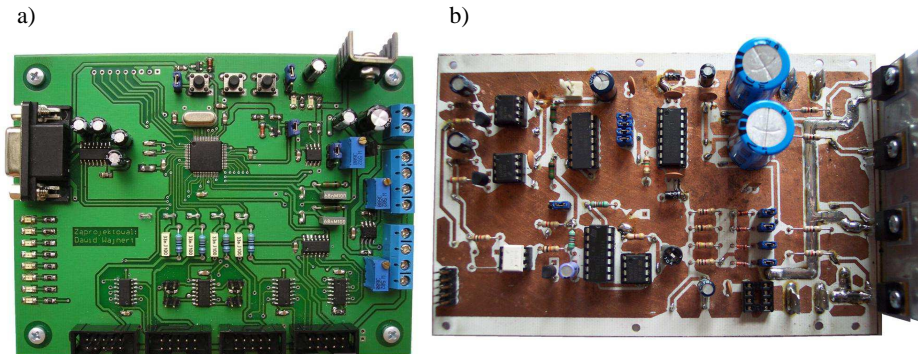


**Fig. 2.** Digital control card (a) and the *h*-bridge amplifier (b) for an AMB12 single axis supplying modules

### Field circuit model of active magnetic bearing

The attractive force acting along the *y* and *x* axes in the magnetic bearings at an operating point can be written as:

$$F_y = k_{iy} i_{cy} + k_{sy} y \tag{1}$$

$$F_x = k_{ix} i_{cx} + k_{sx} x \tag{2}$$

where  $i_{cy}$  and  $i_{cx}$  denote the control current.

The current stiffness coefficient  $k_{iy}$ ,  $k_{ix}$  and position stiffness coefficients  $k_{sy}$ ,  $k_{sx}$  [3, 5] are defined as the partial derivatives of the radial force:

$$k_{iy} = \frac{\mu_0 N^2 A_g i_{by}}{s_0^2}, \quad k_{ix} = \frac{\mu_0 N^2 A_g i_{bx}}{s_0^2} \quad (3)$$

$$k_{sy} = \frac{\mu_0 N^2 A_g i_{by}^2}{s_0^3}, \quad k_{sx} = \frac{\mu_0 N^2 A_g i_{bx}^2}{s_0^3} \quad (4)$$

where  $\mu_0$  is permeability of vacuum,  $N$  is number of turns of the coil,  $A_g$  is the active cross-section area of the pole lamination,  $s_0$  is the nominal air gap for central position of the shaft,  $i_{bx}$  and  $i_{by}$  are the bias currents.

Any elastically supported bodies can undergo mechanical vibrations. They can be described by the motion equation for rigid rotor. Natural vibrations characterize the dynamic behavior of the vibrating structure. Generally, the rotor of a drive is supported radially (elastic or fixed) by two bearings. Under certain assumptions, the axial suspension don't influence on the radial ones. Thus, the axial suspension can be analyzed independently from the radial ones. From Lagrange's equation [1], the equation of motion for rigid rotor can be described by:

$$\mathbf{M} \ddot{\boldsymbol{\zeta}} + \mathbf{K} \boldsymbol{\zeta} + \mathbf{G} \dot{\boldsymbol{\zeta}} = \mathbf{F} \quad (5)$$

where  $\mathbf{M}$  is the mass matrix, which is symmetric and positive defined. The matrix  $\mathbf{G}$  denotes the gyroscopic matrix and  $\mathbf{K}$  is the matrix of stiffness. Vector  $\boldsymbol{\zeta}$  denotes system of state variables. The vector of unbalanced force  $\mathbf{F}$  can be expressed by:

$$\mathbf{F} = \Omega^2 \begin{bmatrix} I_{yz} & I_{zx} \\ -me_z & -me_x \\ I_{zx} & I_{yz} \\ me_x & me_y \end{bmatrix} \begin{bmatrix} \sin \Omega t \\ \cos \Omega t \end{bmatrix} \quad (6)$$

The quantity  $\mathbf{I}$  denotes inertia of the rotor. The unbalance coefficient  $e$  concerns three axes of rotor movement. If matrix  $\mathbf{K}$  is positive defined, the equation (5) is stable for any rotor speeds  $\Omega$ . The force vector  $\mathbf{F}$  depends on the  $t$  time and rotor mass  $m$ .

For relative low frequencies (comparing to the eigenfrequency) and for relatively "very thin" rotors we consider only two equations for the  $x$  and  $y$  axes:

$$\begin{bmatrix} \ddot{x}_c \\ \ddot{y}_c \end{bmatrix} + \begin{bmatrix} \omega^2 & 0 \\ 0 & \omega^2 \end{bmatrix} \begin{bmatrix} x_c \\ y_c \end{bmatrix} = \begin{bmatrix} e\Omega^2 \sin \Omega t \\ e\Omega^2 \cos \Omega t \end{bmatrix} \quad (7)$$

The vector  $\begin{bmatrix} x_c \\ y_c \end{bmatrix}$  denotes coordinates of the shaft position along  $x$  and  $y$  axes and the  $\omega_n^2$  is the

square of the first eigenfrequency of the rotor and can be described as  $\omega_n^2 = \frac{k_n}{m}$ , where  $n = x, y$ .

Taking into account the magnetic field, which is acting on the AMB rotor, the following electromechanical equations should be solved:

$$m\ddot{y} = k_{iy} i_{cy} + k_{sy} y + mg \quad (8a)$$

$$m\ddot{x} = k_{ix}i_{cx} + k_{sx}x \quad (8b)$$

In our work we obtained the stiffness coefficients from the magnetic field analysis of the AMB12 [8]. The active magnetic bearing model has to be expanded by taking into account the electrical properties of the bearing magnets as well as their power amplifiers [6]. Thus, the electrical behavior of the magnetic bearing is described by the matrix equation of the voltage excitation vector  $\mathbf{U}$ :

$$\mathbf{U} = \mathbf{R}\mathbf{i} + \mathbf{L}_d \frac{d\mathbf{i}}{dt} - \mathbf{k}_i \frac{d\mathbf{s}}{dt} \quad (9)$$

where  $\mathbf{R}$  denotes coils resistance matrix,  $\mathbf{L}_d$  is the dynamic inductance matrix. The  $\mathbf{s}$  denotes shaft displacement and takes values of  $x$  or  $y$  position. The current stiffness  $k_{ix}$ ,  $k_{iy}$  are included in stiffness matrix  $\mathbf{k}_i$ . They have been calculated within the numerical analysis of AMB magnetic field [1, 8].

### Calculation results and its measurement verification

The calculations have been carried out for several rotor speeds. In Fig. 3, the rotor trajectories for revolt speed 3000 RPM have been presented. It can be observed, that motor was started at time  $t = 0.17$  s after the activation of the levitation system. The rotor trajectories in the steady state create the curve with elliptic shape. It is due, different of stiffness coefficients in vertical and horizontal directions.

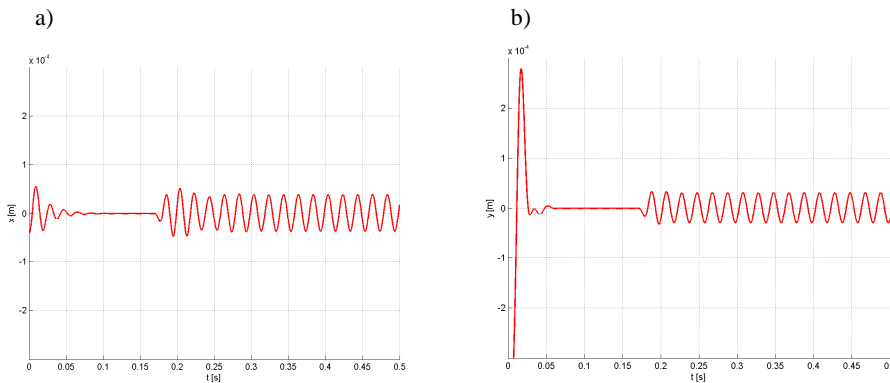


**Fig. 3.** Calculated rotor position changes in AMB12: a) in horizontal direction, b) vertical direction

In Figs. 4 and 5, the measurement verification of calculated rotor trajectories as well as position changes for two rotational speeds, have been presented. The first analysed rotational speed takes value of 3000 RPM. The simulation of the rotor central position has a harmonic character. The amplitude level is about 40  $\mu\text{m}$  (in “ $x$ ” direction) and 30  $\mu\text{m}$  (in “ $y$ ” direction). The measured position waves have periodic character, but they are distorted. Their amplitudes are 52  $\mu\text{m}$  (in “ $x$ ” direction) and 45  $\mu\text{m}$  (in “ $y$ ” direction), respectively.

The rotational speed of 5200 RPM has been assumed for the calculation model. The amplitude level is about 38  $\mu\text{m}$  in “ $x$ ” direction. The measured value differs from the calculated one. In “ $y$ ” direction they are 60  $\mu\text{m}$  and 42  $\mu\text{m}$ , respectively. However, the measured and computed trajectory shapes are very similar.

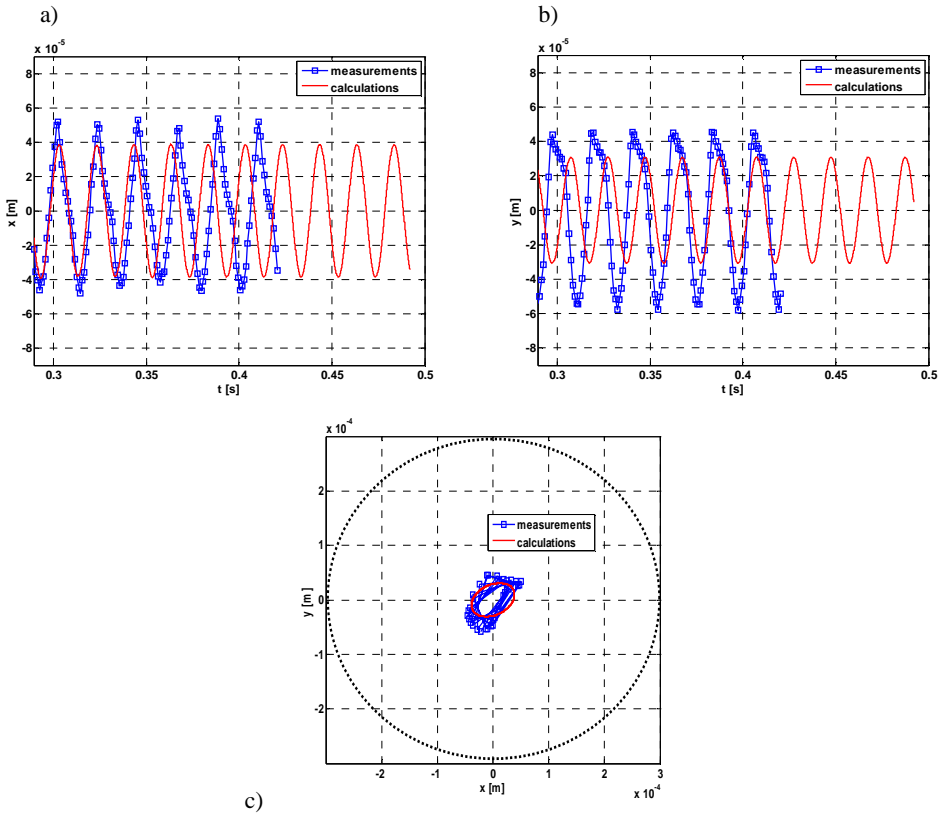


**Fig. 4.** The rotor center position for AMB12 under 3000 RPM: a) horizontal direction, b) vertical direction, c) trajectory in the air gap area

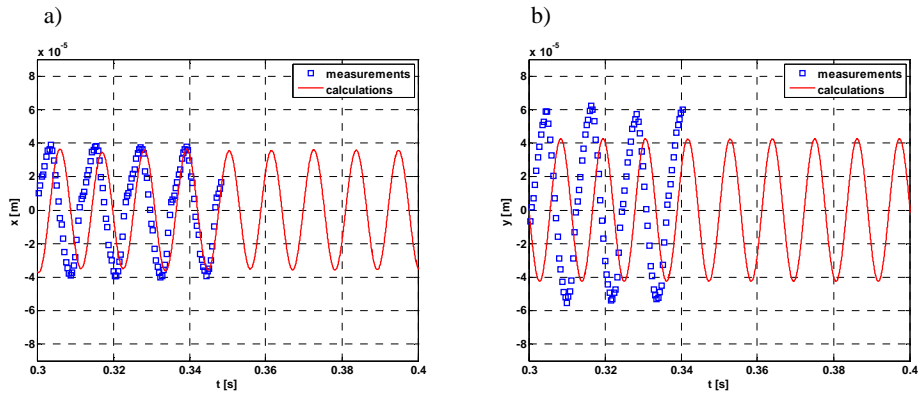


**Fig. 5.** Position changes for AMB12 rotor under 5200 RPM: a) horizontal direction, b) vertical direction

It is visible, that the numerical model is more accurate for higher rotational speeds. It is due to the model simplifications, i. e. the eddy currents neglecting.

### Conclusions

In the work, we have taken a non typical construction of the AMB under consideration. The current and rotor response for the non symmetrical construction have been analyzed.

The calculations of integral field parameters have been carried out with FEM for nonlinear boundary problem. In this work, the magnetic bearing has been analyzed in terms of coupled mathematical models for both the magnetic field analysis and time-stepping model for transients by the solution of the differential equations. Including the PID controller, the analysis of transfer functions and the diagram of the currents as well as their responses, have been modeled for many variants of the studied construction.

From the tests, with the experimental prototype of the AMB we can see that the numerical model can approximate the rotor response. The measured rotor trajectories have been compared with the calculated ones. Some differences for the current and rotor displacement waves arise from numerical model assumptions and measurement inaccuracies. They are also due to errors in positioning of the sensors as well as the assumed stiffness coefficients.

## Acknowledgements

This paper is partially supported by the Polish Ministry of Science and Higher Education under Grant No. N N510 533739 and within the European Social Fund.

## References

- [1] **Schweitzer G., Maslen E.** Magnetic Bearings. Theory, Design and Application to Rotating Machinery. Springer, Berlin, 2009.
- [2] **Antila M.** Electromechanical properties of radial active magnetic bearings. Ph. D. Thesis, Helsinki University of Technology, No. 92, Electrical Engineering Series, Acta Polytechnica Scandinavica, Espoo, Finland, 1998.
- [3] **Gähler C., Förch P.** A precise magnetic bearing exciter for rotordynamic experiments. Proceedings of Fourth International Symposium on Magnetic Bearings, Zürich, Switzerland, August 23–26, 1994, p. 193-200.
- [4] **Gosiewski Z., Falkowski K.** Łożyska Magnetyczne do Maszyn Wirnikowych. Sterowanie i Badanie. Biblioteka Nauk, Instytutu Lotnictwa, Warszawa, 2002, (in Polish).
- [5] **Noh D. M., Maslen E. H., Montie D. T., Kondoleon A.** A simulation model for the analysis of transient magnetic bearing performance. Proceedings of Seventh International Symposium on Magnetic Bearings, Zurich, Switzerland, 2000, p. 177-182.
- [6] **Maslen E.** Magnetic Bearing. Department of Mechanical, Aerospace and Nuclear Engineering, Charlottesville, Virginia, 2000.
- [7] **Gosiewski Z., Falkowski K.** Wielofunkcyjne Łożyska Magnetyczne. Biblioteka Naukowa Instytutu Lotnictwa, Warszawa, 2003, (in Polish).
- [8] **Tomczuk B., Zimon J.** Field determination and calculation of stiffness parameters in an active magnetic bearing (AMB). Solid State Phenomena, Mechatronic Systems and Materials III, Zurich, Switzerland, Vol. 47-149, 2009, p. 125-130.
- [9] Electrical Steel Catalogue: <http://www.stalprodukt.com.pl/>, 19.04.2011.